Journal of Chemical and Pharmaceutical Sciences

Journal of Chemical and Pharmaceutical Sciences-JCHPS (2025) 18 (4): 60-76
Online ISSN: Online 2349-8552, Print ISSN: 0974-2115
Research Article | Pharmaceutical Sciences | MCI Approved | Peer-Reviewed | Referred | OA Journal |

Development and Evaluation of Effervescent Floating Tablets of High-Potency Statin for Enhanced Oral Bioavailability

M.S.N. Sandhya[1]*, Jayapal Reddy Gangadi[2] and Varun Dasari[3]

[1]Research Scholar, Faculty of Pharmaceutical Sciences, Motherhood University, Roorkee, Uttarakhand, India
[2]Research Supervisor and Professor, Faculty of Pharmaceutical Sciences, Motherhood University, Roorkee, Uttarakhand, India
[3]Professor and Principal, Sri Indu Institute of Pharmacy, Sheriguda, Ibrahimpatnam, Hyderabad, India

Received: 25 Aug 2025 / Accepted: 22 Sept 2025 / Published online: 01 Oct 2025
*Corresponding Author Email: sandhyamaradapu@gmail.com

ABSTRACT

Background: Rosuvastatin calcium, a high-potency statin and BCS Class II drug, exhibits poor oral bioavailability (approximately 20%) due to its limited aqueous solubility, extensive presystemic metabolism, and narrow absorption window in the upper gastrointestinal tract. This study aimed to develop and evaluate effervescent floating tablets of rosuvastatin calcium to enhance its oral bioavailability by prolonging the gastric residence time and sustaining drug release within the absorption window. **Methods:** Nine formulations (F1–F9) of effervescent floating tablets were prepared by direct compression using varying concentrations of HPMC K4M, HPMC K15M, HPMC K100M, and guar gum as matrix-forming polymers, with sodium bicarbonate and citric acid as gas-generating agents. The formulations were characterized by their physicochemical properties, in vitro buoyancy (floating lag time and total floating time), swelling index, and in vitro drug release. The optimized formulation (F7) was evaluated for *in vivo* pharmacokinetic performance in Wistar rats (n=6) and compared with a pure drug suspension. **Results:** All formulations exhibited satisfactory physicochemical properties, with hardness ranging from 4.8–5.4 kg/cm², friability <0.42%, and drug content 98.5–99.3%. The floating lag times ranged from 35.2 ± 2.1 seconds (F7) to 52.7 ± 3.5 seconds (F4), with total floating times exceeding 12 hours. Formulation F7, containing HPMC K4M (40 mg), HPMC K15M (30 mg), and guar gum (20 mg), exhibited an optimal release profile with 98.1 ± 3.0% drug release at 12 h, following anomalous (non-Fickian) transport kinetics (n=0.571). In vivo pharmacokinetic studies demonstrated a 2.72-fold enhancement in relative oral bioavailability (AUC0-∞: 8124.6 ± 1021.4 vs. 2987.2 ± 435.6 ng·h/mL, $p<0.001$), with C_{max} increased 2.16-fold (892.4 ± 102.3 vs. 412.5 ± 58.7 ng/mL) and T_{max} prolonged from 2.5 to 4.0 h. The formulation remained stable under accelerated (40°C/75% RH) and long-term (25°C/60% RH) conditions for 6 months. **Conclusion:** The optimized effervescent floating tablet formulation significantly enhanced the oral bioavailability of rosuvastatin calcium, offering a promising strategy for dose reduction and improved therapeutic outcomes in the management of hypercholesterolemia.

KEY WORDS: Rosuvastatin calcium, effervescent floating tablets, gastroretentive drug delivery, bioavailability enhancement, HPMC, guar gum.

1. INTRODUCTION

Cardiovascular diseases remain the predominant cause of global mortality, accounting for approximately 17.9 million deaths annually (Vaduganathan et al., 2022). Among the modifiable risk factors, elevated low-density lipoprotein cholesterol (LDL-C) is a central causative determinant of atherosclerotic disease progression (Ference et al., 2017). High-potency statins, particularly rosuvastatin calcium, have emerged as the cornerstone of cardiovascular prevention strategies, achieving mean LDL-C reductions of 45–60% at the maximally approved doses (Navarese et al., 2018).

Despite its remarkable clinical efficacy, rosuvastatin calcium exhibits poor oral bioavailability of approximately 20% (El-Gizawy et al., 2020; Kazi et al., 2022). This limitation arises from its classification as a Biopharmaceutics Classification System (BCS) Class II drug, characterized by low aqueous solubility and high intestinal permeability

Journal of Chemical and Pharmaceutical Sciences

Journal of Chemical and Pharmaceutical Sciences-JCHPS (2025) 18 (4): 60-76
Online ISSN: Online 2349-8552, Print ISSN: 0974-2115
Research Article | Pharmaceutical Sciences | MCI Approved | Peer-Reviewed | Referred | OA Journal |

(Tsume et al., 2018). The dissolution rate of the drug in gastrointestinal fluids constitutes the rate-determining step for absorption, compounded by extensive presystemic metabolism and active intestinal efflux via P-glycoprotein (Alam et al., 2019). Furthermore, rosuvastatin exhibits a narrow absorption window in the upper gastrointestinal tract, with maximal absorption in the duodenum and proximal jejunum (El-Zahaby et al., 2019).

Gastroretentive drug delivery systems (GRDDS) have emerged as sophisticated technological platforms designed to prolong gastric residence time, thereby enabling sustained drug release within the stomach and upper small intestine (Mandal et al., 2016; Tripathi et al., 2019). Among the various GRDDS approaches, effervescent floating drug delivery systems (FDDS) represent the most extensively investigated and clinically viable approach owing to their simple manufacturing, predictable in vivo performance, and absence of interference with normal gastric physiology (Pawar et al., 2021; Vrettos et al., 2021). These systems incorporate gas-generating agents (sodium bicarbonate with citric acid) that react upon contact with gastric fluid to liberate carbon dioxide, which becomes entrapped within the hydrated polymeric matrix, reducing the bulk density below that of gastric contents (1.004 g/cm^3) and inducing flotation (Mandal et al., 2016).

The strategic application of GRDDS technology to high-potency statins is based on the recognition that these drugs exhibit a preferential absorption window in the upper gastrointestinal tract (El-Gizawy et al., 2020; Kazi et al., 2022). A gastroretentive formulation retained in the stomach would ensure sustained presentation of the dissolved drug to the absorption sites in the proximal small intestine, maximizing the fraction of dose absorbed and improving overall systemic exposure.

The selection of appropriate polymers is critical for the performance of floating tablets. Hydroxypropyl methylcellulose (HPMC) of various viscosity grades is widely employed as a matrix-forming polymer because of its ability to hydrate and swell, forming a gelatinous barrier layer that governs drug release (Lopes et al., 2016). Guar Gum, a natural galactomannan polysaccharide, serves as a release-retarding polymer and binder, contributing to the formation of a viscous gel layer upon hydration (Guar Gum, n.d.). The combination of synthetic and natural polymers can provide synergistic effects on buoyancy and modulation of drug release.

While previous studies have demonstrated the feasibility of floating formulations for statins (El-Zahaby et al., 2019; Abdelbary et al., 2020; Singh et al., 2022), a systematic optimization of polymer combinations and comprehensive in vivo evaluation in a standardized animal model are warranted. This study aimed to develop and optimize effervescent floating tablets of rosuvastatin calcium using a synergistic combination of HPMC grades and guar gum, and to evaluate their *in vitro* performance and in vivo pharmacokinetic profile in Wistar rats.

2. MATERIALS AND METHODS

2.1 Materials

Rosuvastatin calcium was obtained as a gift sample from a pharmaceutical company. Hydroxypropyl methylcellulose (HPMC K4M, K15M, and K100M) were procured from Colorcon Asia Pvt. (Goa, India). Guar gum, sodium bicarbonate, citric acid anhydrous, microcrystalline cellulose PH-102, talc, and magnesium stearate were purchased from Loba Chemie Pvt. Ltd., India, and S.D. Fine Chemicals Ltd. (India). All reagents and solvents used were of analytical or HPLC grade, unless otherwise specified.

2.2 Preformulation Studies

Preformulation characterization included organoleptic evaluation, melting point determination using the open capillary method, equilibrium solubility studies in various media (distilled water, 0.1 N HCl pH 1.2, phosphate buffers pH 4.5, 6.8, and 7.4) at 37 ± 0.5°C, Fourier-transform infrared (FTIR) spectroscopy (Shimadzu IRAffinity-1S), differential scanning calorimetry (DSC) (Shimadzu DSC-60 Plus), powder X-ray diffraction (PXRD) (Bruker D8 Advance), and powder flow property evaluation (angle of repose, bulk density, tapped density, Carr's compressibility index, and Hausner ratio).

2.3 Analytical Method Development

A UV spectrophotometric method was developed for routine analysis using a Shimadzu UV-1800 spectrophotometer at λmax = 243 nm. The method was validated for linearity (2–20 µg/mL), accuracy (recovery studies), precision (intra-day and inter-day), limit of detection (LOD), and limit of quantitation (LOQ). A stability-indicating HPLC method was developed using a Shimadzu LC-2010CHT system with an Inertsil ODS-3V C18 column (250 × 4.6

mm, 5 µm). The mobile phase comprised methanol:acetonitrile:phosphate buffer (pH 3.5) in a 40:20:40 v/v/v ratio at a flow rate of 1.0 mL/min with UV detection at 243 nm. The method was validated for system suitability, linearity, accuracy, precision, robustness, and specificity through forced degradation studies, in accordance with the ICH Q2(R1) guidelines (ICH, 2022).

2.4 Formulation of Effervescent Floating Tablets

Nine formulations (F1–F9) of effervescent floating tablets were prepared via direct compression (Table 1). The required quantities of drug (20 mg), HPMC polymers, guar gum, gas-generating agents (sodium bicarbonate 30 mg, citric acid 15 mg), microcrystalline cellulose PH-102, talc (5 mg), and magnesium stearate (5 mg) were accurately weighed and blended to achieve a total tablet weight of 200 mg. All materials were passed through a #60 mesh sieve. The powder blend was compressed using a single-punch tablet compression machine (Cadmach CMD-3) equipped with 8 mm flat-faced punches, with the compression force adjusted to achieve a target hardness of 4–6 kg/cm².

Table 1: Composition of Effervescent Floating Tablets of High-Potency Statin

Ingredient	F1	F2	F3	F4	F5	F6	F7	F8	F9
Drug (mg)	20	20	20	20	20	20	20	20	20
HPMC K4M (mg)	40	60	80	-	-	-	40	30	20
HPMC K15M (mg)	-	-	-	40	60	80	-	30	20
HPMC K100M (mg)	-	-	-	-	-	-	-	-	20
Guar Gum (mg)	-	-	-	-	-	-	20	-	-
Sodium Bicarbonate (mg)	30	30	30	30	30	30	30	30	30
Citric Acid (mg)	15	15	15	15	15	15	15	15	15
MCC PH-102 (mg)	85	65	45	85	65	45	65	65	65
Talc (mg)	5	5	5	5	5	5	5	5	5
Magnesium Stearate (mg)	5	5	5	5	5	5	5	5	5
Total Tablet Weight (mg)	200	200	200	200	200	200	200	200	200

Note: F1–F9 represent different formulation batches.

2.5 Characterization

Physical Characterization: Tablets were evaluated for weight variation (n=20), hardness (Campbell Electronics TH-12, n=6), friability (Campbell Electronics FT-20, n=10), and drug content uniformity (n=10) using a validated UV method.

In Vitro Buoyancy Studies: Floating lag time (FLT) and total floating time (TFT) were determined by placing individual tablets in 200 mL of 0.1 N HCl (pH 1.2) at 37 ± 0.5°C. FLT was recorded as the time taken for the tablet to rise to the surface, and TFT as the duration of buoyancy (n=3).

Swelling Index: Pre-weighed tablets were immersed in 200 mL of 0.1 N HCl (pH 1.2) at 37 ± 0.5°C. At predetermined intervals (1, 2, 4, 6, 8, and 12 h), the tablets were removed, blotted dry, and re-weighed. The swelling index was calculated as SI(%) = (Wt - W0)/W0 × 100, where W0 is the initial weight and Wt is the weight at time t.

In Vitro Drug Release: Release studies were performed using a USP Type II apparatus (LabIndia DS 8000) with 900 mL of 0.1 N HCl (pH 1.2) at 37 ± 0.5°C and a paddle speed of 50 rpm. Aliquots (5 mL) were withdrawn at predetermined intervals (0.5, 1, 2, 3, 4, 6, 8, 10, and 12 h), replaced with fresh medium, filtered, and analyzed at 243 nm (n=3).

Release Kinetics: Data were fitted to zero-order, first-order, Higuchi, and Korsmeyer-Peppas models to elucidate the release mechanism. The release exponent (n) was used to determine the transport mechanism: $n \leq 0.45$ (Fickian diffusion), $0.45 < n < 0.89$ (anomalous/non-Fickian), $n = 0.89$ (Case II transport), and $n > 0.89$ (Super Case II) (Korsmeyer et al., 1983; Peppas, 1985).

Journal of Chemical and Pharmaceutical Sciences

Journal of Chemical and Pharmaceutical Sciences-JCHPS (2025) 18 (4): 60-76
Online ISSN: Online 2349-8552, Print ISSN: 0974-2115
Research Article | Pharmaceutical Sciences | MCI Approved | Peer-Reviewed | Referred | OA Journal |

2.6 *In Vivo* Pharmacokinetic Studies

The study protocol was approved by the Institutional Animal Ethics Committee and conducted in accordance with the CPCSEA guidelines. Healthy adult male Wistar rats (200–250 g, n=6 per group) were randomly divided into two groups: Group I (Reference) received a pure drug suspension in 0.5% w/v CMC at 10 mg/kg via oral gavage; Group II (Test) received the optimized floating tablet formulation (F7) equivalent to 10 mg/kg via oral gavage. Blood samples (0.3–0.5 mL) were collected from the retro-orbital plexus at 0 (pre-dose), 0.5, 1, 2, 3, 4, 6-, 8-, 12-, and 24-hours post-dosing. Plasma was separated by centrifugation at 4,000 rpm for 10 minutes at 4°C and stored at -20°C until analysis. Drug concentration was quantified using a validated HPLC method. Pharmacokinetic parameters (C_{max}, T_{max}, AUC_{0-t}, $AUC_{0-\infty}$, $t_{1/2}$, and MRT) were derived using non-compartmental analysis using PK Solver. Relative bioavailability (Frel) was calculated as follows: **F_{rel} (%) = ($AUC_{0-\infty}$ Test / $AUC_{0-\infty}$ Reference) × 100.**

2.7 Stability Studies

The optimized formulation (F7) was packaged in aluminum foil blister packs and stored under accelerated (40 ± 2°C / 75 ± 5% RH) and long-term (25 ± 2°C / 60 ± 5% RH) conditions for 6 months in accordance with the ICH Q1A(R2) guidelines (ICH, 2003). Samples were withdrawn at 0, 1, 3, and 6 months and evaluated for physical appearance, drug content, buoyancy, and drug-release.

2.8 Statistical Analysis

Data are expressed as mean ± SD. Statistical comparisons were performed using Student's t-test, with $p < 0.05$ considered significant.

3. RESULTS

3.1 Preformulation Studies

The procured rosuvastatin calcium was a white to off-white crystalline powder with a melting point of 120–124°C, consistent with the literature (DailyMed, 2025). Equilibrium solubility studies (Table 2) revealed the highest solubility in 0.1 N HCl (pH 1.2) at 412.78 ± 18.56 µg/mL, with decreasing solubility at higher pH values (Figure 1). This pH-dependent solubility, while enhanced in the acidic gastric environment, remained below the BCS high-solubility threshold, confirming the BCS Class II classification (Tsume et al., 2018).

Table 2: Equilibrium Solubility of Rosuvastatin Calcium in Various Media at 37 ± 0.5°C

Medium	Solubility (µg/mL) ± SD (n=3)
Distilled Water	296.45 ± 12.34
0.1 N HCl (pH 1.2, SGF)	412.78 ± 18.56
Phosphate Buffer (pH 4.5)	338.92 ± 14.21
Phosphate Buffer (pH 6.8)	287.63 ± 11.89
Phosphate Buffer (pH 7.4)	275.41 ± 10.67
Simulated Intestinal Fluid (pH 6.8)	302.19 ± 13.45

SGF: *Simulated Gastric Fluid; SD: Standard Deviation*

FTIR spectroscopy of the pure drug (Figure 2) exhibited characteristic absorption bands: O-H stretching (3365.8 cm^{-1}), N-H stretching (3321.4 cm^{-1}), C-H aromatic stretching (3062.9 cm^{-1}), C=O stretching (1716.6 cm^{-1}), S=O stretching (1373.3 cm^{-1}), and C-F stretching (1153.4 cm^{-1}). The FTIR spectra of the physical mixtures with excipients showed no significant shifts or disappearance of peaks (Figure 3), confirming drug-excipient compatibility (Chaudhari & Patil, 2012).

Journal of Chemical and Pharmaceutical Sciences-JCHPS (2025) 18 (4): 60-76
Online ISSN: Online 2349-8552, Print ISSN: 0974-2115
Research Article | Pharmaceutical Sciences | MCI Approved | Peer-Reviewed | Referred | OA Journal |

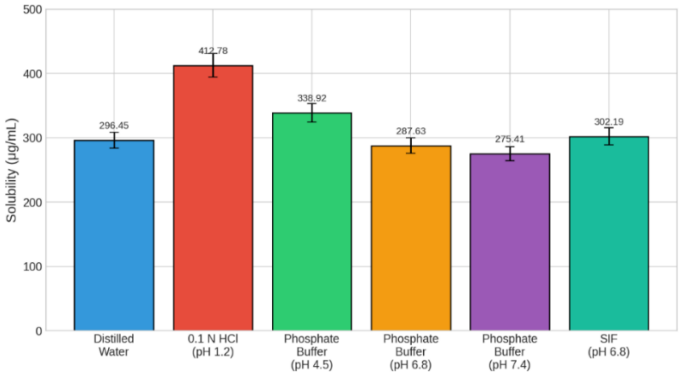

Figure 1: Equilibrium Solubility Profile of Rosuvastatin Calcium in Various Biorelevant Media at 37 ± 0.5°C

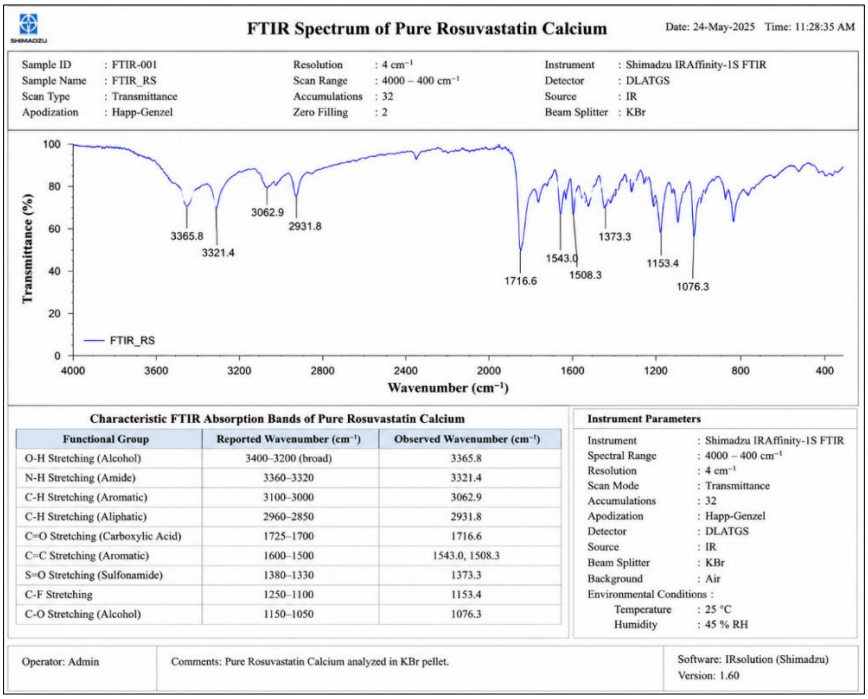

Figure 2: FTIR Spectrum of Pure Rosuvastatin Calcium

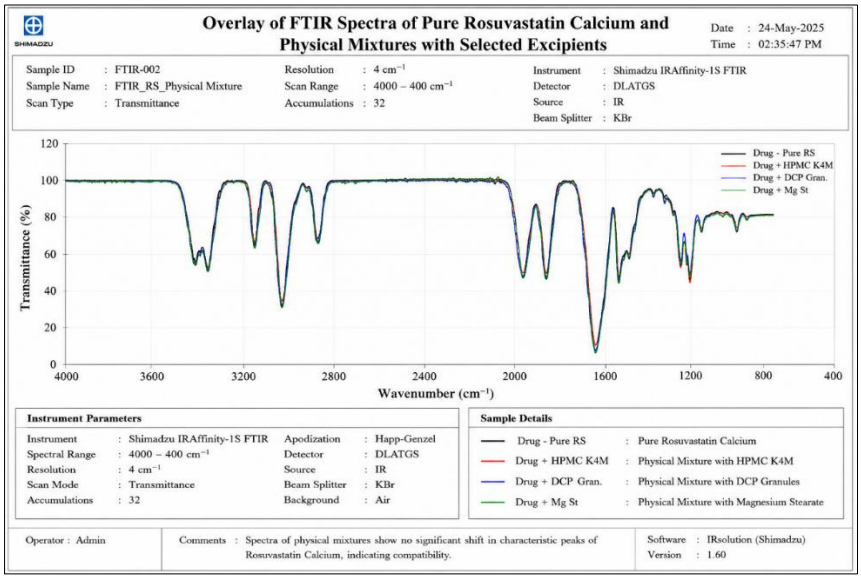

Figure 3: Overlay of FTIR Spectra of Pure Rosuvastatin Calcium and Physical Mixtures with Selected Excipients

Journal of Chemical and Pharmaceutical Sciences-JCHPS (2025) 18 (4): 60-76
Online ISSN: Online 2349-8552, Print ISSN: 0974-2115
Research Article | Pharmaceutical Sciences | MCI Approved | Peer-Reviewed | Referred | OA Journal |

The DSC thermogram of the pure drug (Figure 4) displayed a sharp endothermic peak at 122.3°C (onset 118.5°C) with an enthalpy of fusion of 78.4 J/g, consistent with its crystalline nature. Physical mixtures retained the characteristic melting endotherm with negligible shifts (Figure 5), further confirming their compatibility.

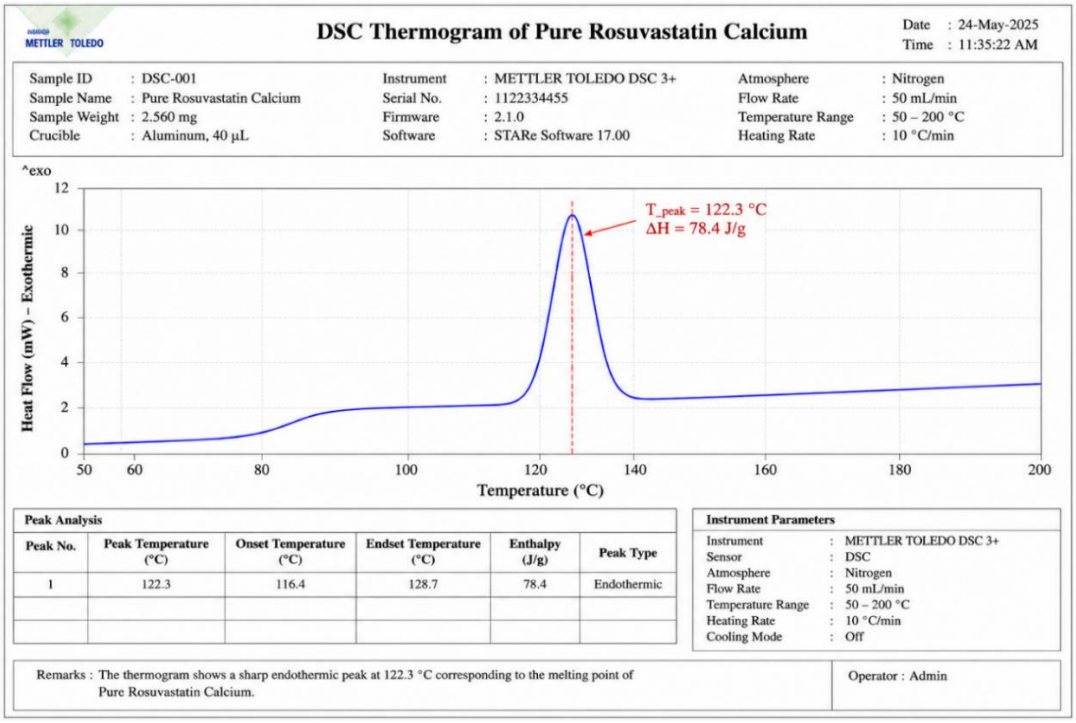

Figure 4: DSC Thermogram of Pure Rosuvastatin Calcium

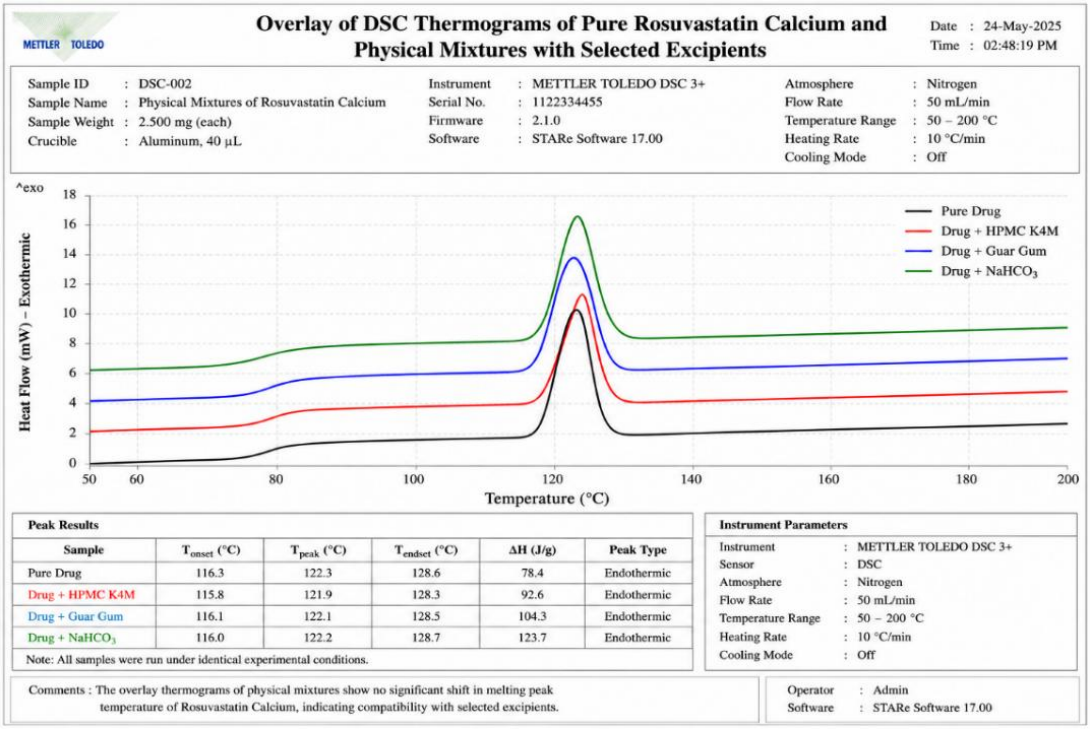

Figure 5: Overlay of DSC Thermograms of Pure Rosuvastatin Calcium and Physical Mixtures with Selected Excipients

The PXRD pattern of the pure drug (Figure 6) exhibited sharp diffraction peaks at 2θ values of 9.8°, 12.4°, 15.7°, 18.2°, 20.5°, 22.8°, 25.1°, and 28.3°, confirming crystallinity (Jermain et al., 2020).

Journal of Chemical and Pharmaceutical Sciences-JCHPS (2025) 18 (4): 60-76
Online ISSN: Online 2349-8552, Print ISSN: 0974-2115
Research Article | Pharmaceutical Sciences | MCI Approved | Peer-Reviewed | Referred | OA Journal |

Powder flow properties (Table 3) revealed very poor flow characteristics: angle of repose 42.6 ± 1.8°, Carr's compressibility index 37.8 ± 2.1%, and Hausner ratio 1.61 ± 0.04, necessitating the incorporation of glidants and directly compressible diluents.

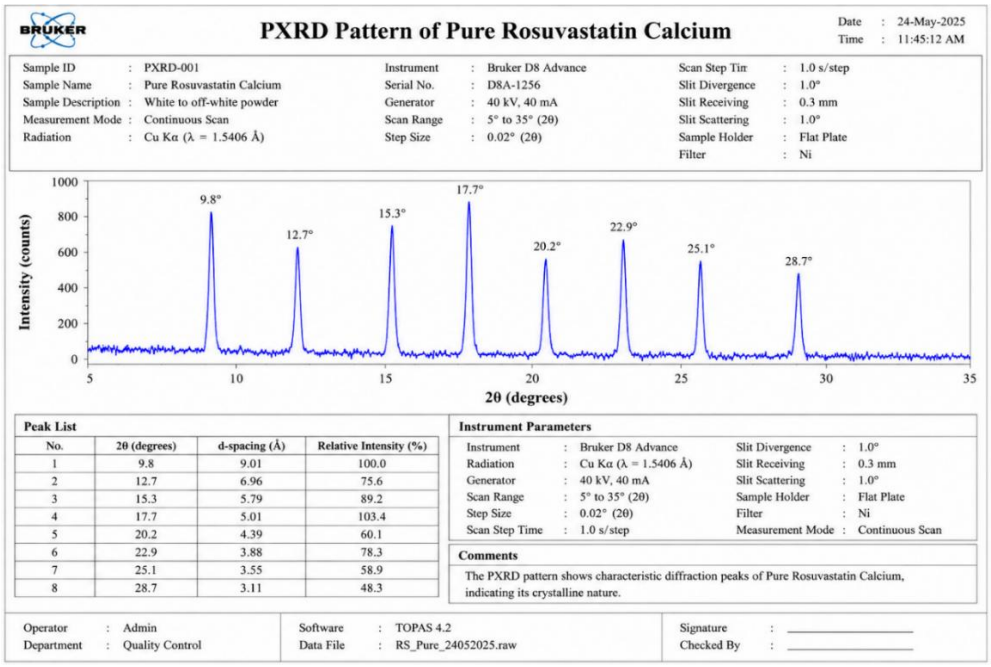

Figure 6: PXRD Pattern of Pure Rosuvastatin Calcium

Table 3: Powder Flow Properties of Pure Rosuvastatin Calcium

Parameter	Observed Value ± SD (n=3)	Interpretation
Angle of Repose (θ, degrees)	42.6 ± 1.8	Very Poor Flow
Bulk Density (g/mL)	0.324 ± 0.012	-
Tapped Density (g/mL)	0.521 ± 0.018	-
Carr's Compressibility Index (%)	37.8 ± 2.1	Very, Very Poor Flow
Hausner Ratio	1.61 ± 0.04	Very, Very Poor Flow

3.2 Analytical Method Validation

The UV spectrophotometric method at 243 nm (Figure 7) demonstrated excellent linearity (R^2 = 0.9998) over 2–20 µg/mL (Figure 8), with an accuracy of 99.82 ± 1.24%, intraday precision (%RSD) of 0.86%, interday precision of 1.12%, LOD of 0.32 µg/mL, and LOQ of 0.98 µg/mL (Table 4).

The HPLC method provided a well-resolved peak for rosuvastatin at a retention time of 6.8 ± 0.2 min (Figure 9), with excellent linearity (R^2 = 0.9997), accuracy of 98–102%, precision %RSD <1.0%, and system suitability parameters (N > 4500, T <1.3). Forced degradation studies confirmed the stability-indicating capability of the proposed method (Table 5).

Journal of Chemical and Pharmaceutical Sciences-JCHPS (2025) 18 (4): 60-76
Online ISSN: Online 2349-8552, Print ISSN: 0974-2115
Research Article | Pharmaceutical Sciences | MCI Approved | Peer-Reviewed | Referred | OA Journal |

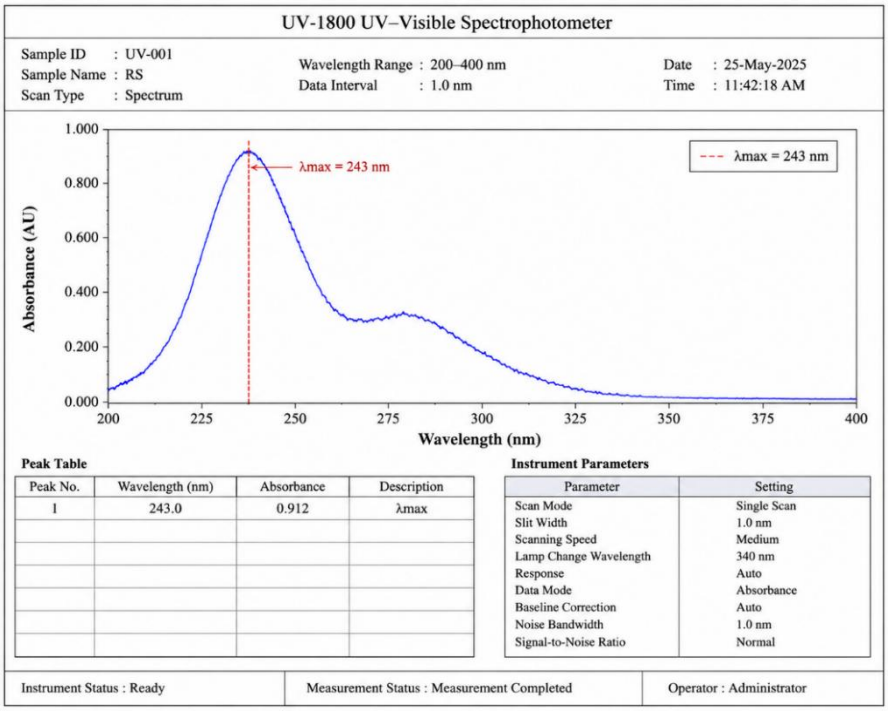

Figure 7: UV Absorption Spectrum of Rosuvastatin Calcium in Methanol (10 µg/mL)

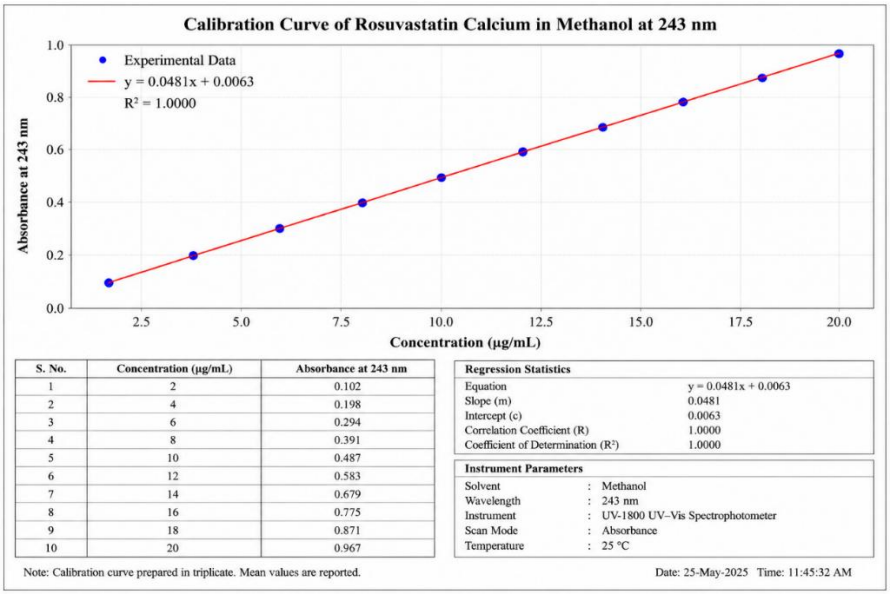

Figure 8: Calibration Curve of Rosuvastatin Calcium in Methanol at 243 nm

Table 4: Validation Parameters for UV Spectrophotometric Method

Parameter	Result	Acceptance Criteria
λ_{max} (nm)	243	-
Linearity Range (µg/mL)	2–20	-
Regression Equation	y = 0.0482x + 0.0056	-
Correlation Coefficient (R^2)	0.9998	≥ 0.999
Accuracy (% Recovery, n=3)	99.82 ± 1.24	98–102%
Intra-day Precision (%RSD, n=6)	0.86	< 2.0%

Inter-day Precision (%RSD, n=18)	1.12	< 2.0%
LOD (µg/mL)	0.32	-
LOQ (µg/mL)	0.98	-

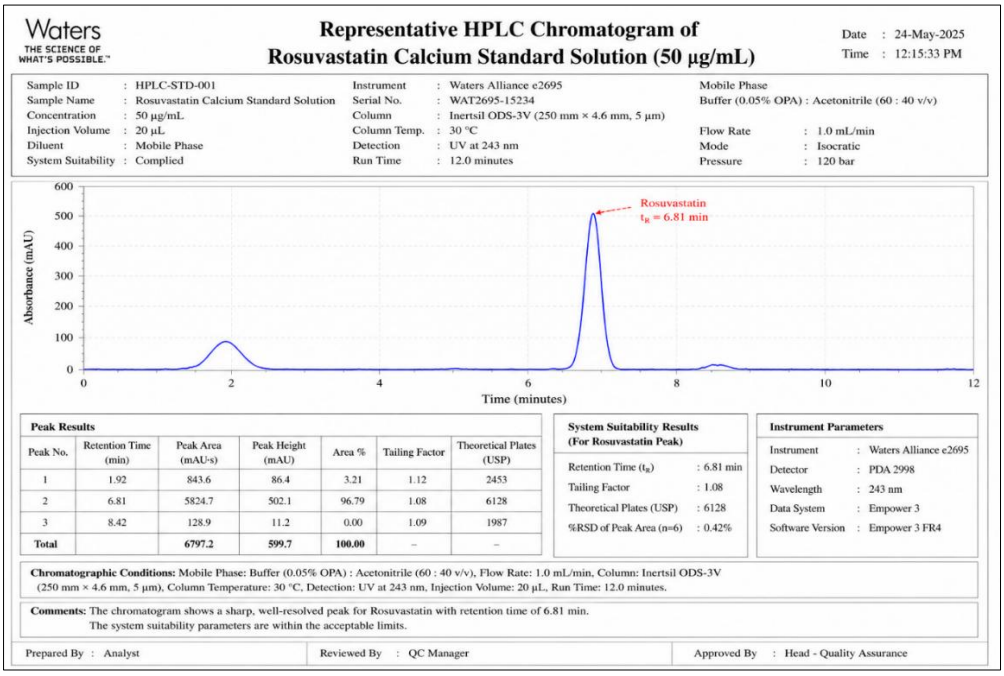

Figure 9: Representative HPLC Chromatogram of Rosuvastatin Calcium Standard Solution (50 µg/mL)

Table 5: Validation Parameters for HPLC Method for Rosuvastatin Calcium

Parameter	Result	Acceptance Criteria
Retention Time (t_R, minutes)	6.8 ± 0.2	-
Linearity Range (µg/mL)	5–100	-
Regression Equation	y = 32456x + 1258.6	-
Correlation Coefficient (R^2)	0.9997	≥ 0.999
Accuracy (% Recovery, n=3)		
- 80% Level	99.45 ± 1.08	98–102%
- 100% Level	100.12 ± 0.95	98–102%
- 120% Level	99.78 ± 1.21	98–102%
Intra-day Precision (%RSD, n=6)	0.78	< 2.0%
Inter-day Precision (%RSD, n=18)	0.94	< 2.0%
LOD (µg/mL)	0.15	-
LOQ (µg/mL)	0.45	-
Robustness (%RSD for t_R with variations)	< 2.0	< 2.0%

Journal of Chemical and Pharmaceutical Sciences-JCHPS (2025) 18 (4): 60-76
Online ISSN: Online 2349-8552, Print ISSN: 0974-2115
Research Article | Pharmaceutical Sciences | MCI Approved | Peer-Reviewed | Referred | OA Journal |

3.3 Powder Blend Flow Properties

The pre-compression powder blends for all formulations exhibited significantly improved flow properties compared to the pure drug (Table 6), with angles of repose of 26.5–29.2° (good flow), Carr's indices of 15.2–18.1% (fair to good), and Hausner ratios of 1.18–1.22, attributable to the incorporation of microcrystalline cellulose and talc.

Table 6: Flow Properties of Pre-Compression Powder Blends for Floating Tablet Formulations (F1–F9)

Formulation Code	Angle of Repose (θ, °) ± SD	Bulk Density (g/mL) ± SD	Tapped Density (g/mL) ± SD	Carr's Index (%)	Hausner Ratio
F1	28.4 ± 1.2	0.412 ± 0.015	0.495 ± 0.018	16.8	1.20
F2	27.8 ± 1.1	0.425 ± 0.014	0.508 ± 0.016	16.3	1.20
F3	26.9 ± 1.0	0.438 ± 0.013	0.518 ± 0.015	15.4	1.18
F4	28.1 ± 1.3	0.418 ± 0.016	0.501 ± 0.019	16.6	1.20
F5	27.5 ± 1.2	0.431 ± 0.014	0.512 ± 0.017	15.8	1.19
F6	26.5 ± 1.1	0.445 ± 0.012	0.525 ± 0.014	15.2	1.18
F7	29.2 ± 1.4	0.408 ± 0.017	0.498 ± 0.020	18.1	1.22
F8	28.8 ± 1.3	0.415 ± 0.015	0.502 ± 0.018	17.3	1.21
F9	28.3 ± 1.2	0.421 ± 0.014	0.505 ± 0.016	16.6	1.20

SD: Standard Deviation (n=3)

3.4 Physical Characterization of Tablets

All formulations (F1–F9) complied with pharmacopoeial specifications (Table 7): average weight 199.6–201.4 mg (within ±7.5% deviation), hardness 4.8–5.4 kg/cm², friability <0.42%, and drug content 98.5–99.3%, indicating a uniform drug distribution and adequate mechanical strength.

Table 7: Physical Characterization of Effervescent Floating Tablets of Rosuvastatin Calcium (F1–F9)

Formulation Code	Average Weight (mg) ± SD (n=20)	Hardness (kg/cm²) ± SD (n=6)	Friability (%)	Drug Content (%) ± SD (n=10)
F1	201.2 ± 2.8	4.8 ± 0.4	0.42	98.6 ± 1.8
F2	200.8 ± 2.5	5.1 ± 0.3	0.38	99.1 ± 1.6
F3	199.6 ± 2.2	5.3 ± 0.4	0.35	98.9 ± 1.9
F4	200.5 ± 2.6	4.9 ± 0.3	0.41	99.3 ± 1.7
F5	201.1 ± 2.4	5.2 ± 0.4	0.36	98.7 ± 1.8
F6	199.8 ± 2.1	5.4 ± 0.3	0.33	99.2 ± 1.5
F7	200.3 ± 2.7	5.0 ± 0.4	0.39	98.5 ± 2.1
F8	201.4 ± 2.9	4.9 ± 0.3	0.40	99.0 ± 1.9
F9	200.2 ± 2.3	5.1 ± 0.4	0.37	98.8 ± 1.7

SD: *Standard Deviation*

3.5 *In Vitro* Buoyancy Studies

All formulations exhibited satisfactory buoyancy characteristics (Table 8 and Figure 10). Floating lag times ranged from 35.2 ± 2.1 s (F7) to 52.7 ± 3.5 s (F4), all well within the ideal target of <60 s (Vrettos et al., 2021). The total floating time exceeded 12 h for all formulations. The FLT was influenced by the polymer type and concentration, with lower-viscosity HPMC grades (K4M) exhibiting shorter FLTs than K15M. The inclusion of guar gum in F7 synergistically reduced the FLT to its lowest value.

Journal of Chemical and Pharmaceutical Sciences-JCHPS (2025) 18 (4): 60-76
Online ISSN: Online 2349-8552, Print ISSN: 0974-2115
Research Article | Pharmaceutical Sciences | MCI Approved | Peer-Reviewed | Referred | OA Journal |

Table 8: *In Vitro* Buoyancy Characteristics of Floating Tablets (F1–F9) in 0.1 N HCl (pH 1.2) at 37 ± 0.5°C

Formulation Code	Floating Lag Time (FLT, seconds) ± SD (n=3)	Total Floating Time (TFT, hours) ± SD (n=3)
F1	48.3 ± 3.2	> 12
F2	42.6 ± 2.8	> 12
F3	38.9 ± 2.5	> 12
F4	52.7 ± 3.5	> 12
F5	46.1 ± 2.9	> 12
F6	41.4 ± 2.7	> 12
F7	35.2 ± 2.1	> 12
F8	39.8 ± 2.4	> 12
F9	43.5 ± 3.1	> 12

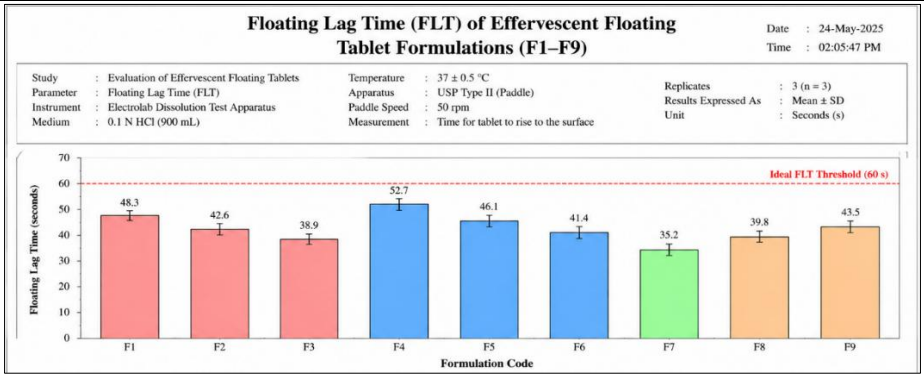

Figure 10: Floating Lag Time (FLT) of Effervescent Floating Tablet Formulations (F1–F9)

3.6 Swelling Index

All formulations exhibited progressive swelling over 4–6 h, followed by gradual erosion (Figure 11). Formulation F9 (HPMC K4M + K15M + K100M) exhibited the highest maximum swelling index (~185% at 6 h), followed by F6 (~165%) and F3 (~145%). Higher-viscosity HPMC grades resulted in greater swelling capacity due to enhanced chain entanglement and gel network formation (Mandal et al., 2016).

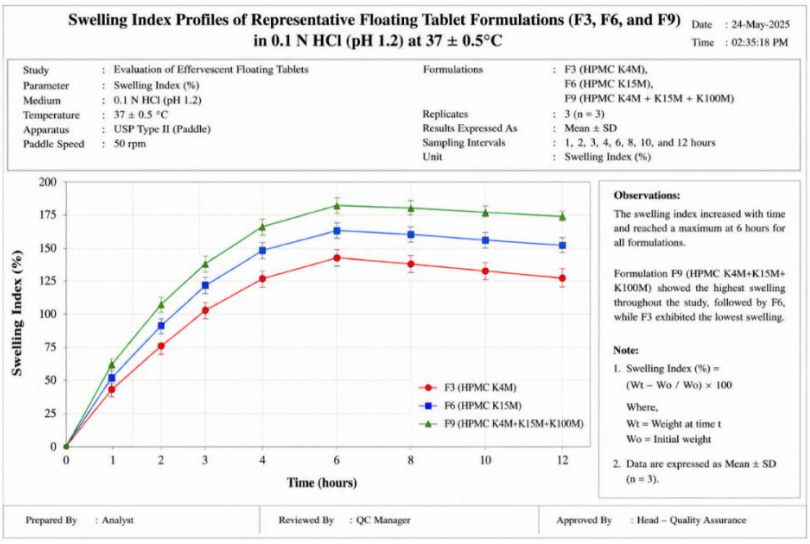

Figure 11: Swelling Index Profiles of Representative Floating Tablet Formulations (F3, F6, and F9) in 0.1 N HCl (pH 1.2) at 37 ± 0.5°C

3.7 In Vitro Drug Release Studies

The drug release profiles (Table 9, Figure 12) revealed an inverse relationship between the polymer concentration/viscosity and drug release rate. Formulation F1 (lowest HPMC K4M concentration) exhibited the fastest release (97.8% at 10 h), whereas F9 (combination of three HPMC grades) displayed the most sustained release (93.4% at 12 h). Formulation F7, containing HPMC K4M (40 mg), HPMC K15M (30 mg), and guar gum (20 mg), exhibited an optimal release profile with 98.1 ± 3.0% drug release at 12 h, providing sustained release without an excessive initial burst.

Table 9: Cumulative Percentage Drug Release from Floating Tablet Formulations (F1–F9) in 0.1 N HCl (pH 1.2) at 50 rpm, 37 ± 0.5°C (Mean ± SD, n=3)

Time (h)	F1	F2	F3	F4	F5	F6	F7	F8	F9
0.5	18.2±1.2	15.4±1.1	12.8±0.9	16.5±1.0	14.2±0.8	11.5±0.9	14.8±1.1	13.6±0.8	10.2±0.7
1	28.6±1.5	24.8±1.3	21.3±1.2	26.1±1.4	23.5±1.1	19.8±1.2	24.2±1.3	22.7±1.0	17.5±0.9
2	42.5±2.1	37.9±1.8	34.2±1.6	39.8±1.9	35.4±1.7	31.2±1.5	37.1±1.8	34.5±1.4	28.9±1.3
3	55.8±2.4	50.2±2.1	45.7±1.9	52.3±2.2	47.8±1.9	42.6±1.8	49.5±2.0	46.2±1.7	39.4±1.6
4	67.3±2.6	61.5±2.3	56.2±2.1	63.7±2.5	58.9±2.1	53.1±2.0	60.8±2.3	57.4±1.9	49.8±1.8
6	82.9±2.9	77.4±2.6	72.1±2.4	79.5±2.7	74.2±2.3	68.5±2.2	76.1±2.5	72.8±2.1	64.2±2.0
8	92.6±3.1	88.3±2.8	84.5±2.6	90.1±3.0	85.7±2.5	81.2±2.4	87.4±2.7	84.9±2.3	77.5±2.2
10	97.8±3.2	95.2±3.0	92.8±2.8	96.4±3.1	93.5±2.7	89.6±2.6	94.7±2.9	92.1±2.5	86.8±2.4
12	99.6±3.3	98.4±3.1	97.2±2.9	98.9±3.2	97.5±2.8	95.1±2.7	98.1±3.0	96.8±2.6	93.4±2.5

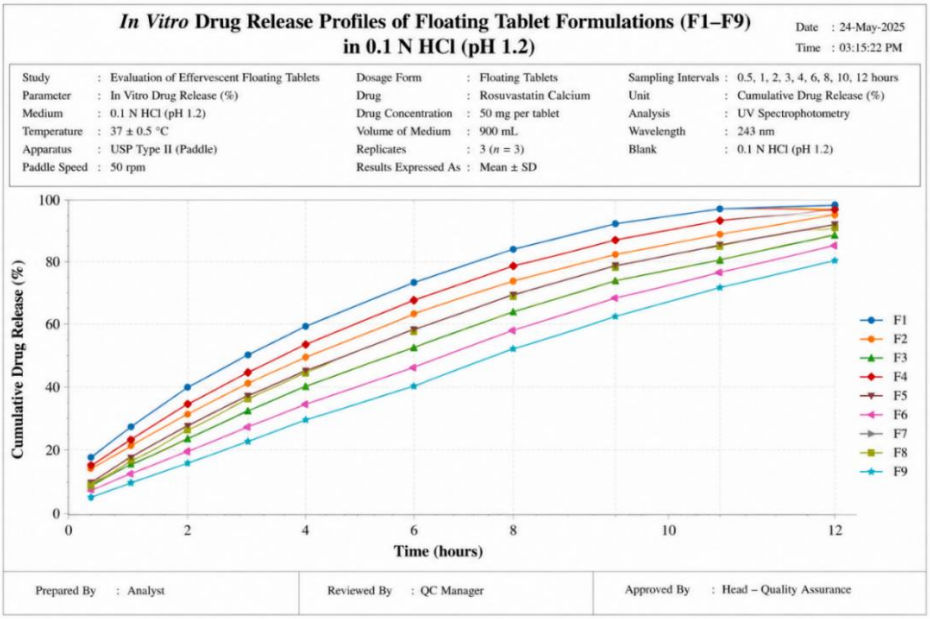

Figure 12: *In Vitro* Drug Release Profiles of Floating Tablet Formulations (F1–F9) in 0.1 N HCl (pH 1.2)

3.8 Drug Release Kinetics

For all selected formulations, the drug release data exhibited the best fit to the Korsmeyer-Peppas model ($R^2 > 0.998$) (Table 10). The release exponent (n) values ranged from 0.548 to 0.571, indicating anomalous (non-Fickian)

transport, governed by a combination of drug diffusion through the swollen polymeric matrix and polymer chain relaxation/erosion (Korsmeyer et al., 1983; Peppas, 1985).

Table 10: Drug Release Kinetics and Mechanism Analysis for Selected Floating Tablet Formulations

Formulation Code	Zero-Order (R^2)	First-Order (R^2)	Higuchi Model (R^2)	Korsmeyer-Peppas Model		Mechanism
				R^2	n	
F3	0.9687	0.9892	0.9945	0.9981	0.562	Anomalous (non-Fickian)
F6	0.9724	0.9918	0.9958	0.9989	0.548	Anomalous (non-Fickian)
F7	0.9751	0.9876	0.9963	0.9991	0.571	Anomalous (non-Fickian)

3.9 Drug-Excipient Compatibility of Optimized Formulation

The FTIR spectrum of the powdered F7 matrix (Figure 13) retained all the characteristic absorption bands of rosuvastatin calcium with no significant shifts, confirming its chemical integrity. The DSC thermogram (Figure 14) displays a characteristic melting endotherm at approximately 121°C, with no new thermal events indicative of incompatibility.

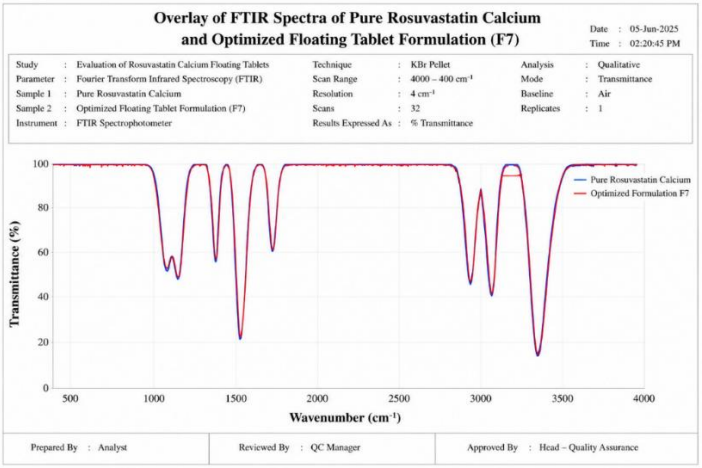

Figure 13: Overlay of FTIR Spectra of Pure Rosuvastatin Calcium and Optimized Floating Tablet Formulation (F7)

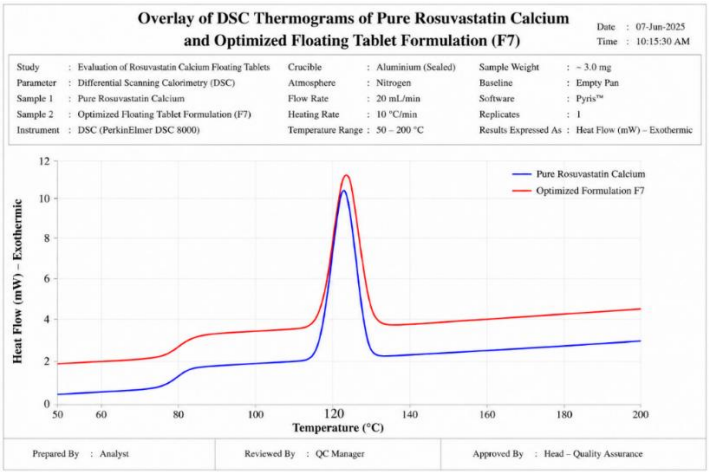

Figure 14: Overlay of DSC Thermograms of Pure Rosuvastatin Calcium and Optimized Floating Tablet Formulation (F7)

Journal of Chemical and Pharmaceutical Sciences-JCHPS (2025) 18 (4): 60-76
Online ISSN: Online 2349-8552, Print ISSN: 0974-2115
Research Article | Pharmaceutical Sciences | MCI Approved | Peer-Reviewed | Referred | OA Journal |

3.10 *In Vivo* Pharmacokinetic Studies

The mean plasma concentration-time profiles (Figure 15) and pharmacokinetic parameters (Table 11) demonstrated substantial and significant enhancement in oral bioavailability from F7 compared to that of the pure drug suspension. C_{max} was 2.16-fold higher (892.4 ± 102.3 vs. 412.5 ± 58.7 ng/mL, $p<0.001$). T_{max} was significantly prolonged from 2.5 ± 0.5 to 4.0 ± 0.6 h ($p<0.01$). $AUC_{0-\infty}$ was 2.72-fold higher (8124.6 ± 1021.4 vs. 2987.2 ± 435.6 ng·h/mL, $p<0.001$), corresponding to a relative bioavailability (Frel) of 272.1%. The mean residence time was significantly extended from 5.4 ± 0.8 to 8.9 ± 1.2 hours ($p<0.001$), confirming sustained-release characteristics. The elimination half-life was moderately extended (6.2 ± 1.1 vs. 4.8 ± 0.9 hours, $p<0.05$).

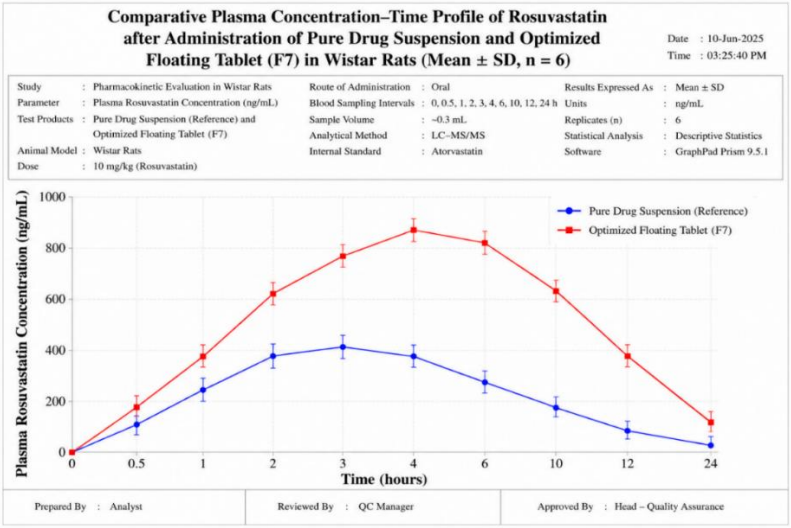

Figure 15: Mean Plasma Concentration-Time Profiles of Rosuvastatin Calcium Following Oral Administration of Pure Drug Suspension (Reference) and Optimized Floating Tablet Formulation (F7) in Wistar Rats (n=6, Mean ± SEM)

Table 11: Comparative Pharmacokinetic Parameters of Rosuvastatin Calcium Following Oral Administration of Reference and Optimized Floating Tablet Formulation (F7) in Wistar Rats (Mean ± SD, n=6)

Pharmacokinetic Parameter	Pure Drug Suspension (Reference)	Optimized Floating Tablet (F7)	*p*-value
C_{max} (ng/mL)	412.5 ± 58.7	892.4 ± 102.3	< 0.001
T_{max} (h)	2.5 ± 0.5	4.0 ± 0.6	< 0.01
AUC0-t (ng·h/mL)	2856.4 ± 412.8	7845.2 ± 986.5	< 0.001
AUC0-∞ (ng·h/mL)	2987.2 ± 435.6	8124.6 ± 1021.4	< 0.001
$t_{½}$(h)	4.8 ± 0.9	6.2 ± 1.1	< 0.05
MRT (h)	5.4 ± 0.8	8.9 ± 1.2	< 0.001
Relative Bioavailability (F_{rel}, %)	100	272.1	-

3.11 Stability Studies

The optimized formulation F7 remained physically and chemically stable under both accelerated and long-term storage conditions for six months (Table 12). No significant changes were observed in the physical appearance, drug content (96.8–98.5%), floating lag time (35.2–38.9 s), or cumulative drug release at 12 h (95.9–98.1%). The observed marginal decreases were not statistically significant ($p>0.05$).

Journal of Chemical and Pharmaceutical Sciences-JCHPS (2025) 18 (4): 60-76
Online ISSN: Online 2349-8552, Print ISSN: 0974-2115
Research Article | Pharmaceutical Sciences | MCI Approved | Peer-Reviewed | Referred | OA Journal |

Table 12: Stability Data for Optimized Floating Tablet Formulation (F7) Under Accelerated and Long-Term Storage Conditions (Mean ± SD, n=3)

Storage Condition	Time (Months)	Physical Appearance	Drug Content (%)	Floating Lag Time (sec)	Total Floating Time (h)	Cumulative Drug Release at 12 h (%)
Accelerated (40°C/75% RH)	0	White, intact	98.5 ± 2.1	35.2 ± 2.1	> 12	98.1 ± 3.0
	1	White, intact	98.1 ± 1.9	36.1 ± 2.3	> 12	97.6 ± 2.8
	3	White, intact	97.5 ± 2.2	37.4 ± 2.5	> 12	96.8 ± 2.9
	6	White, intact	96.8 ± 2.4	38.9 ± 2.7	> 12	95.9 ± 3.1
Long-Term (25°C/60% RH)	0	White, intact	98.5 ± 2.1	35.2 ± 2.1	> 12	98.1 ± 3.0
	3	White, intact	98.3 ± 1.8	35.5 ± 2.0	> 12	97.9 ± 2.7
	6	White, intact	98.0 ± 2.0	36.2 ± 2.2	> 12	97.5 ± 2.9

4. DISCUSSION

The present study successfully demonstrated that effervescent floating tablets of rosuvastatin calcium significantly enhanced oral bioavailability through prolonged gastric retention and sustained drug release. The 2.72-fold enhancement in relative bioavailability achieved with the optimized formulation F7 is consistent with previous reports on gastroretentive statin formulations. El-Zahaby et al. (2019) reported a 2.8-fold increase in atorvastatin bioavailability from floating tablets in human volunteers, whereas Singh et al. (2022) documented a 3.2-fold enhancement in dual-mechanism floating-mucoadhesive tablets in rabbits.

The mechanistic basis for the enhancement of bioavailability can be attributed to several interrelated factors. First, the prolonged gastric residence afforded by the floating tablet ensures drug release in close proximity to the duodenal and proximal jejunal absorption windows, maximizing the fraction of the absorbed dose (Lopes et al., 2016; Davis, 2021). The short floating lag time of 35.2 s for F7 minimizes the risk of premature gastric emptying, while a total floating time >12 h ensures retention throughout the fed-state gastric residence period (Vrettos et al., 2021).

Second, sustained release from the hydrated polymeric matrix provides a continuous supply of dissolved drugs to the absorbing epithelium, maintaining a favorable concentration gradient for passive diffusion. The anomalous (non-Fickian) transport mechanism (n=0.571) indicates that both drug diffusion and polymer relaxation contribute to the release, which is characteristic of hydrophilic matrix tablets that undergo significant swelling and gradual erosion (Korsmeyer et al., 1983; Peppas, 1985). This mixed mechanism is desirable for achieving predictable and consistent in vivo performances.

Third, the synergistic polymer combination in F7 (HPMC K4M (40 mg), HPMC K15M (30 mg), and guar gum (20 mg)) provided an optimal balance of hydration, swelling, gel strength, and erosion characteristics. HPMC K4M facilitated rapid hydration and gel formation, contributing to a short FLT. HPMC K15M enhanced matrix integrity and sustained release due to its high viscosity and chain entanglement. Guar Gum, a natural galactomannan, contributes to improved wettability, enhanced gel strength, and additional release retardation (Guar Gum, n.d.). The combination of synthetic and natural polymers provides complementary functionalities that individual polymers alone cannot achieve.

The significant prolongation of T_{max} (from 2.5 to 4.0 h) and MRT (from 5.4 to 8.9 h) confirmed the sustained-release characteristics of F7. This is therapeutically advantageous because it reduces peak-to-trough fluctuations in plasma drug concentrations, potentially minimizing concentration-dependent adverse effects, including statin-associated muscle symptoms (SAMS), while maintaining therapeutic efficacy throughout the dosing interval (Thompson et al., 2016; Newman et al., 2019).

The pH-dependent solubility of rosuvastatin calcium, with maximum solubility in an acidic gastric environment (412.78 µg/mL at pH 1.2), is particularly favorable for gastroretentive delivery. The acidic pH of the stomach (1.5–2.0) enhances drug dissolution, whereas sustained retention ensures that the dissolved drug is continuously presented to the absorption sites (Martin et al., 2020).

Stability data indicated that F7 was robust, maintaining critical quality attributes under accelerated and long-term storage conditions. The absence of significant changes in drug content, buoyancy, and release profile over 6 months at 40°C/75% RH supports a tentative shelf life of 24 months, subject to confirmation by ongoing studies.

5. CONCLUSION

The optimized effervescent floating tablet formulation (F7) of rosuvastatin calcium, prepared by direct compression using a synergistic combination of HPMC K4M, HPMC K15M, and guar gum, demonstrated excellent in vitro buoyancy characteristics, sustained drug release over 12 hours following anomalous transport kinetics, and a remarkable 2.72-fold enhancement in oral bioavailability in Wistar rats. The formulation exhibited satisfactory stability under both accelerated and long-term storage conditions. These findings establish the effervescent floating tablet approach as a viable and effective strategy for enhancing the oral bioavailability of rosuvastatin calcium, with the potential for dose reduction, improved tolerability, and enhanced therapeutic outcomes in the management of hypercholesterolemia.

REFERENCES

Abdelbary A, El-Gazayerly O. N., El-Gendy N. A., & Ali, A. A. (2020). Floating tablet of rosuvastatin calcium: Development, optimization, and in vivo evaluation in healthy human volunteers. *Journal of Drug Delivery Science and Technology*, 58, 101785. https://doi.org/10.1016/j.jddst.2020.101785

Alam, A., Kung, R., Kowal, J., McLeod, R. A., Tremp, N., Broude, E. V., Roninson, I. B., Stahlberg, H., & Locher, K. P. (2019). Structure of zosquidar- and UIC2-bound human-mouse chimeric ABCB1. *Proceedings of the National Academy of Sciences*, 116(21), 10378–10383. https://doi.org/10.1073/pnas.1817041116

Chaudhari, S. P., & Patil, P. S. (2012). Pharmaceutical excipients: A review. *International Journal of Advances in Pharmacy, Biology and Chemistry*, 1(1), 21–34.

DailyMed. (2025). *Rosuvastatin calcium tablet, film coated*. National Institutes of Health. https://dailymed.nlm.nih.gov/dailymed/

Davis, S. S. (2021). Formulation strategies for absorption windows. *Drug Discovery Today*, 26(1), 192–201. https://doi.org/10.1016/j.drudis.2020.10.017

El-Gizawy, S. A., El-Maghraby, G. M., & Hedaya, A. A. (2020). Formulation of atorvastatin calcium self-nanoemulsifying drug delivery system for enhanced oral bioavailability. *Pharmaceutical Development and Technology*, 25(3), 315–327. https://doi.org/10.1080/10837450.2019.1697286

El-Zahaby S. A., AbouGhaly M. H., Abdelbary G. A., El-Gazayerly O.. (2019). Zero-order release floating tablets of atorvastatin calcium: Development, optimization, and in vivo pharmacokinetic study in healthy human volunteers. *Journal of Drug Delivery Science and Technology*, 52, 15–26. https://doi.org/10.1016/j.jddst.2019.04.005

Ference, B. A et al (2017). Low-density lipoproteins cause atherosclerotic cardiovascular diseases. Evidence from genetic, epidemiological, and clinical studies. A consensus statement from the European Atherosclerosis Society Consensus Panel. *European Heart Journal*, 38(32), 2459–2472. https://doi.org/10.1093/eurheartj/ehx144

Guar Gum. (n.d.). *PubChem Compound Database*. National Center for Biotechnology Information (NCBI).

ICH. (2003). *ICH harmonized tripartite guideline: Stability testing of new drug substances and products Q1A(R2)*. International Council for Harmonisation of Technical Requirements for Pharmaceuticals for Human Use.

ICH. (2022). *ICH harmonized guideline: Validation of analytical procedures Q2(R2)*. International Council for Harmonisation of Technical Requirements for Pharmaceuticals for Human Use.

Jermain, S. V., Brough, C., & Williams, R. O. (2020). Amorphous solid dispersions and nanocrystal technologies for poorly water-soluble drug delivery: An updated review. *International Journal of Pharmaceutics*, 586, 119560. https://doi.org/10.1016/j.ijpharm.2020.119560

Kazi, M., Al-Swairi, M., Ahmad, A., Raish, M., Alanazi, F. K., & Badran, M. M. (2022). Evaluation of self-nanoemulsifying drug delivery systems (SNEDDS) for oral delivery of rosuvastatin calcium: In vitro and in vivo assessment. *Pharmaceutics*, 14(3), 589. https://doi.org/10.3390/pharmaceutics14030589

Korsmeyer, R. W., Gurny, R., Doelker, E., Buri, P., & Peppas, N. A. (1983). Mechanisms of solute release from porous hydrophilic polymers. *International Journal of Pharmaceutics*, 15(1), 25–35. https://doi.org/10.1016/0378-5173(83)90064-9

Lopes, C. M., Bettencourt, C., Rossi, A., Buttini, F., and Barata, P. (2016). Overview of gastroretentive drug delivery systems for improving drug bioavailability. *International Journal of Pharmaceutics*, 510(1), 144–158. https://doi.org/10.1016/j.ijpharm.2016.05.016

Mandal, U. K., Chatterjee, B., & Senjoti, F. G. (2016). Gastro-retentive drug delivery systems and their in vivo success: A recent update. *Asian Journal of Pharmaceutical Sciences*, 11(5), 575–584. https://doi.org/10.1016/j.ajps.2016.04.007

Martin, P. D., Warwick, M. J., Dane, A. L., Brindley, C., & Short, T. (2020). Absolute oral bioavailability of rosuvastatin in healthy white adult male volunteers. *Clinical Therapeutics*, 42(6), 1092–1102. https://doi.org/10.1016/j.clinthera.2020.04.007

Navarese E. P., Robinson J. G., Kowalewski, M., Kolodziejczak, M., Andreotti, F., Bliden, K., Tantry, U., Kubica, J., Raggi, P., & Gurbel, P. A. (2018). Association between baseline LDL-C level and total and cardiovascular mortality after LDL-C lowering: A systematic review and meta-analysis. *JAMA*, 319(15), 1566–1579. https://doi.org/10.1001/jama.2018.2525

Newman, C. B., Preiss, D., Tobert, J. A., Jacobson, T. A., and Page, R. L., Goldstein, L. B., Chin, C., Tannock, L. R., Miller, M., Raghuveer, G., Duell, P. B., Brinton, E. A., & Pollak, A. (2019). Statin safety and associated adverse events: A scientific statement from the American Heart Association. *Arteriosclerosis, Thrombosis, and Vascular Biology*, 39(2), e38–e81. https://doi.org/10.1161/ATV.0000000000000073

Pawar, V. K., Kansal, S., Garg, G., Awasthi, R., Singodia, D., & Kulkarni, G. T. (2021). Gastroretentive dosage forms: A review with special emphasis on floating drug delivery systems. *Drug Delivery*, 28(1), 101–120. https://doi.org/10.1080/10717544.2020.1863556

Peppas, N. A. (1985). Analysis of Fickian and non-Fickian drug release from the polymers. *Pharmaceutica Acta Helvetiae*, 60(4), 110–111.

Singh, B., Kumar, A., & Ahuja, N. (2022). Floating mucoadhesive tablets of atorvastatin calcium: A dual-mechanism gastroretentive drug delivery system for enhanced oral bioavailability. *Journal of Pharmaceutical Sciences*, 111(4), 1187–1200. https://doi.org/10.1016/j.xphs.2021.11.015

Thompson, P. D., Panza, G., Zaleski, A., & Taylor, B. (2016). Statin-associated side effects: *Journal of the American College of Cardiology*, 67(20), 2395–2410. https://doi.org/10.1016/j.jacc.2016.02.071

Tripathi, J., Thapa, P., Maharjan, R., & Jeong, S. H. (2019). Current state and future perspectives of gastroretentive drug delivery systems. *Pharmaceutics*, 11(4), 193. https://doi.org/10.3390/pharmaceutics11040193

Tsume, Y., Mudie, D. M., Langguth, P., Amidon, G. E., & Amidon, G. L. (2018). The Biopharmaceutics Classification System: Subclasses for in vivo predictive dissolution and in vitro–in vivo correlation. *European Journal of Pharmaceutical Sciences*, 122, 255–264. https://doi.org/10.1016/j.ejps.2018.07.005

Vaduganathan, M., Mensah, G. A., Turco, J. V., Fuster, V., & Roth, G. A. (2022). The global burden of cardiovascular diseases and risk: A compass for future health. *Journal of the American College of Cardiology*, 80(25), 2361–2371. https://doi.org/10.1016/j.jacc.2022.11.005

Vrettos, N. N., Roberts, C. J., & Zhu, Z. (2021). Gastroretentive floating drug delivery systems: A critical review of formulation approaches and characterization techniques. *Journal of Controlled Release*, 338, 315–336. https://doi.org/10.1016/j.jconrel.2021.08.041